Hindawi
Journal of Renewable Energy
Volume 2019, Article ID 3684284, 11 pages
https://doi.org/10.1155/2019/3684284

Research Article

A Comparison Analysis of the Experimental and Theoretical Power Output of a Hybrid Photovoltaic Cell

Damasen Ikwaba Paul

The Open University of Tanzania, Faculty of Science, Technology and Environmental Studie, P.O. Box 23409, Dar es Salaam, Tanzania

Correspondence should be addressed to Damasen Ikwaba Paul; paul.ikwaba@out.ac.tz

Received 5 November 2018; Revised 12 February 2019; Accepted 25 February 2019; Published 25 March 2019

Academic Editor: Senthilarasu Sundaram

In this paper, experimental and theoretical power output of a hybrid photovoltaic cell were analysed and compared for three different weather conditions (clear sky, partial cloudy, and overcast days). The hybrid photovoltaic cell consisted of low efficiency cell (mono-crystalline) and strips of Bosch M 2BB mono-crystalline cell as high efficiency cell. The current and voltage for the experimental results were measured by using optimal resistive load method. Theoretical daily power output of the hybrid PV cell was calculated based on the hourly incident energy on each section, the size of the section, and the electrical conversion efficiency of each section. The hybrid cell was evaluated within a low-concentrating symmetric compound parabolic concentrator suitable for building integration and was tilted at 54°. It was found that the theoretical daily power output on a clear sky, partial cloudy, and overcast days was higher than the experimental results by 136%, 109%, and 121%, respectively. The discrepancy was due to losses as the result of connecting wires series resistance effect, operating temperature effect, and the consequence of the fixed resistive load. However, it was the value of the optimal resistive load that had much impact on the experimental power output. To eliminate the restriction of the optimal resistive load on the experimental results, it is recommended to use data acquisition systems such as photovoltaic peak power measuring device 6020C 6020C or Keithley 2651A source-meter.

1. Introduction

One of the greatest challenges facing the world today is breaking fossil fuel dependence and promoting the development of new and renewable sources of energy that can supplement and replace the diminishing resources of fossil fuels. This is due to the fact that climate change, rise of price for conventional energy sources, and energy insecurity are the greatest threats to human, economy, and political stability, respectively [1]. Solar energy is clearly one of the most promising prospects to these problems since it is non-pollutant [2, 3], renewable [3], and available everywhere in the world although with varying intensity [3]. Solar power is more than capable of fulfilling the electricity demands of the whole world [3]. On the earth's surface, solar energy is converted into electrical energy through a process called photovoltaic effect [4–6].

Electrical energy from photovoltaic (PV) can be generated from flat panel or concentrated panel. In both cases, the evaluation of the performance of the PV panel is determined from the values of current and voltage [7–9]. This is due to the fact that most important parameters such as short-circuit current (I_{SC}), open-circuit voltage (V_{OC}), current at maximum power point (I_{MMP}), voltage at maximum power point (V_{MMP}), and power output at maximum power point (P_{MMP}) can be extracted from the current against voltage (I–V) curve [7–9]. In practical situation, current and voltage are experimentally measured by using either data acquisition systems [10, 11] or optimal resistance method [12–16]. The main advantage of using a data acquisition system is that it continuously adjusts the electrical load to achieve the maximum possible output power, thus presenting accurate value of power output. On the other hand, the use of optimal resistance method leads to power output losses for solar radiation outside the operating range of the optimal load value [17, 18]. The reason is that optimal load value does not automatically adjust the load to ensure maximum power output as solar irradiance varies throughout the day [18, 19].

On the other hand, the performance of a PV system can be evaluated theoretically through simulation [20–22] or

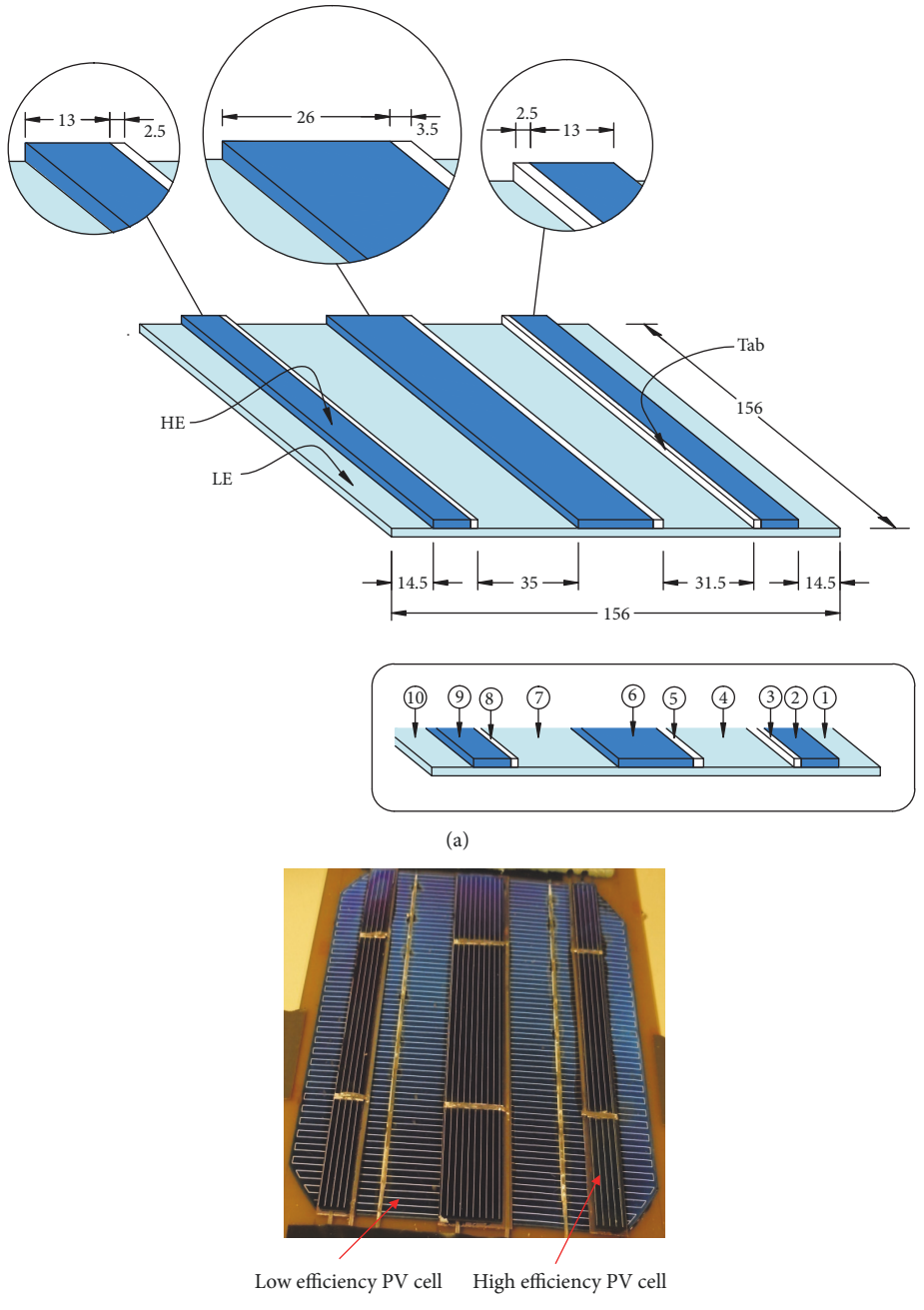

Figure 1: The hybrid PV cell consists of high efficiency (HE) cell and low efficiency (LE) cell: (a) detailed design (b) and complete fabricated cell, adapted from Paul and Smyth [28].

numerical calculations [23, 24]. Theoretically, it is possible to test different aspects such as design, layout, materials, and operation conditions prior to implementation of the actual system [25, 26]. In this way, actual experimentation can be avoided which is costly and time consuming. In addition, theoretical results are more accurate than experimental because the effects of optical, series resistance, non-uniform illumination, and high operating cell temperature are excluded [27].

In an effort to improve the performance of the PV modules against non-uniform illumination, recently Paul and Smyth [28] designed, fabricated, and experimentally tested a hybrid PV cell consisting of high efficiency cell and low efficiency cell. The layout design and a complete fabricated hybrid PV cell are shown in Figure 1. The hybrid PV cell was evaluated within a low-concentrating symmetric two-dimensional (2D) compound parabolic concentrator (CPC) suitable for integration into the building envelope [29]. The motivation for such a design was to obtain high electrical power at low cost for the reason that the area occupied by high quality cell (which is expensive) was less (33%) than the area occupied by economical low efficiency cell

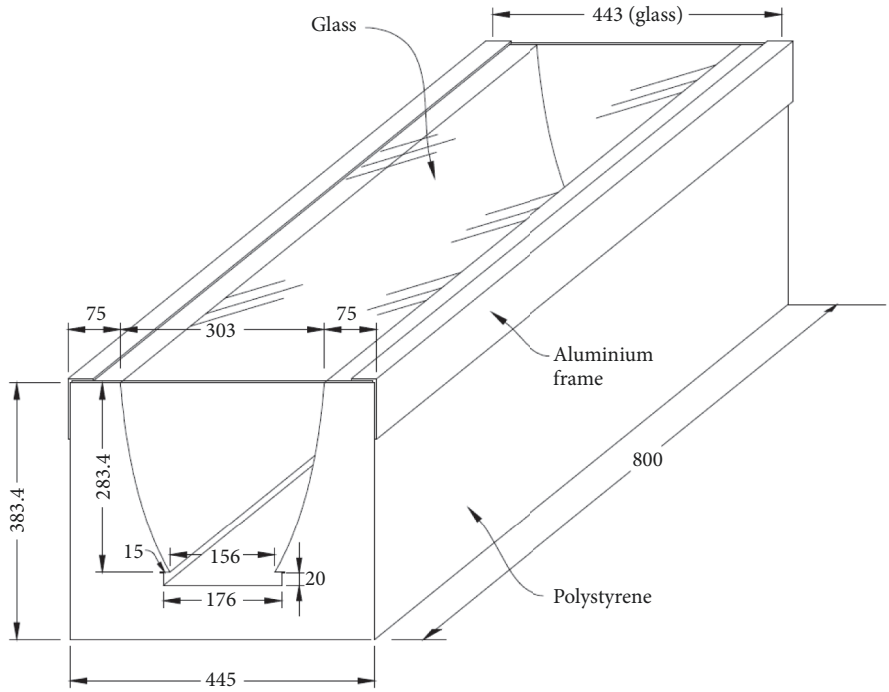

Figure 2: Detailed design dimensions of a symmetric 2D CPC and fabrication materials (all dimensions are in mm) [28].

(62%). However, outdoor experimental results indicated that the power output produced by the hybrid PV cell on a clear sky day, partial cloudy day, and overcast day was higher than that of standard PV cell only by 12%, 10%, and 9%, respectively. Considering the difference in conversion efficiencies between the two PV cells (17.5% for high efficiency cell against 12% of low efficiency cell) and the advantage of non-uniform illumination on the performance of the hybrid PV cell [28], the reported results were below expectation.

Therefore, the objective of this study was to carry out a detailed theoretical analysis of the power output generated by the hybrid PV cell under the three weather conditions (clear sky, partial cloudy, and overcast days) and compare the results with the experimental values. Underlying reasons were provided for the observed differences between the experimental and the theoretical results.

2. Materials and Methods

2.1. Specifications of the Compound Parabolic Concentrator. In this study, a truncated symmetric 2D CPC with dimensions and fabrication materials shown in Figure 2 was used [28]. The design of this collector was based on the standard procedures described by Paul [30]. The collector had an acceptance half-angle of 30° and after truncation, the entrance width was reduced to 303 mm and the exit width remained 156 mm, making a geometric concentration ratio of 1.94. Aluminium sheet with reflectivity of 0.91 and opti-white glass with extinction coefficient of 4 m^{-1} were used as reflector material and aperture cover, respectively.

2.2. Performance Parameters of the Hybrid Photovoltaic Cell. The hybrid PV cell used in this study was designed and fabricated by Paul and Smyth [28] and reproduced in this work as Figure 1. This PV cell consisted of low efficiency (LE) cell and high efficiency (HE) cell. The low efficiency cell was mono-crystalline solar cell with performance parameters listed in Table 1 [31] whereas the high efficiency cell was Bosch M 2BB mono-crystalline cell with performance parameters listed in Table 2 [32].

2.3. Experimental Test Procedure. The experimental results used in this work are from Paul and Smyth [28]. The measurements for these results were conducted during a clear sky day, partial cloudy day, and overcast day. These days were deliberately selected so that the results could represent the variations in solar irradiance typical in any given year. The experimental facilities were set at the Centre for Sustainable Technology Laboratory, Ulster University, Jordanstown Campus. The CPC (with a hybrid PV cell) was oriented North–South and tilted at 54° (Figure 3). One pyranometer was fixed on the aperture of the CPC as shown on Figure 3 so as to measure global solar radiation while diffuse irradiance was measured by a pyranometer with a diffuser ring (not shown in Figure 3). Then, beam solar irradiance was obtained by subtracting diffuse irradiance from global irradiance. The ambient and cell temperatures were measured by 561 Fluke Infrared and Contact Thermometer while wind speed was measured by a digital anemometer fixed on the aperture of the CPC as shown in Figure 3. The current and voltage were measured by using fixed resistive load method [18] where the optimal value was 102 mΩ.

Table 1: Physical and electrical properties of mono-crystalline PV cell [31]. Electrical data applied for standard test conditions (1,000 W/m^2, AM[2]1.5 spectrum and 25°C).

Physical characteristics					
Dimensions	156 mm x 156 mm (±0.5 mm)				
Average thickness	200 μm (±40 μm)				
Front contacts (–)	2 mm busbar (silver), textured, silicon nitride antireflective coating				
Back contacts (+)	4.5 mm busbar (silver), full-surface aluminum BSF				
Electrical characteristics					
V_{OC} (mV)	I_{SC} (mA)	V_{MPP} (mV)	I_{MPP} (mA)	P_{MPP} (W)	η[3] (%)
523	6250	493	5923	2.92	12.00

[2]AM is air mass.
[3]η is solar cell conversion efficiency.

Table 2: Physical and electrical properties of the Bosch M 2BB PV cell [32]. Electrical data applied for standard test conditions (1,000 W/m^2, AM1.5 spectrum and 25°C).

Physical characteristics					
Dimensions	156 mm x 156 mm (±0.5 mm)				
Average thickness	200 μm (±40 μm)				
Front contacts (–)	2 mm busbar (silver), textured, silicon nitride antireflective coating				
Back contacts (+)	4.5 mm busbar (silver), full-surface aluminum BSF				
Electrical characteristics					
V_{OC} (mV)	I_{SC} (mA)	V_{MPP} (mV)	I_{MPP} (mA)	P_{MPP} (Wp)	η (%)
616	8861	511	8270	4.23	17.50
Temperature coefficients	α[4] (I_{SC}): +0.03 %/K, β[5] (V_{OC}): –0.37 %/K, γ[6] (P_{MPP}): –0.49 %/K				

[4]α is the temperature coefficient of the short–circuit current.
[5]β is the temperature coefficient of the open–circuit voltage.
[6]γ is the temperature coefficient of the power output at maximum power point.

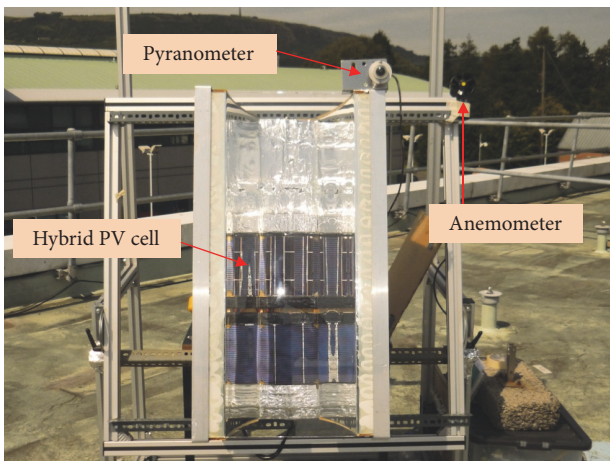

Figure 3: Outdoor experimental set-up [28].

2.4. Calculations of Theoretical Daily Power Output. The theoretical power output of the hybrid PV cell (P_{Daily}) shown in Figure 1(a), equivalent to the total time of the experimented test, was calculated based on the hourly incident energy on each section of the cell, the size of the section and the electrical conversion efficiency of each section using (1).

$$P_{Daily} = \sum P_{Hour} = \sum_{i=1}^{i=10} P_{Hour}(i) \quad (1)$$

where

$$P_{Hour}(i) = G_B \times C_B \times A_i \times \eta_i + G_D \times C_D \times A_i \times \eta_i \quad (2)$$

where $i = 1, 2, 3, \ldots, 10$ is the number of sections forming the hybrid PV cell, G_B, G_D, C_B, and C_D are the beam solar irradiance on the aperture of the CPC, diffuse solar irradiance on the aperture of the CPC, beam energy concentration on the ith section of the hybrid PV cell, and diffuse energy concentration on the ith section of the PV cell, respectively. $P_{Hour}(i)$ is the hourly electrical power produced by the ith section of the hybrid cell, P_{Hour} is the total electrical power of the hybrid PV cell at every hour, A_i is the area of the ith section of the hybrid PV cell, and η_i is the conversion efficiency of the ith section of the hybrid PV cell. The beam/diffuse energy concentration factor is the product of beam/diffuse optical efficiency and the aperture area of the CPC. The optical efficiency at each incidence angle was determined by using simulation program [33].

For sections of the hybrid PV cell occupied by connecting tabs as shown in Figure 1(a), $\eta_i = 0$ thus, $P_{Hour}(i) = 0$.

In calculating the power output, beam and diffuse solar irradiance that were measured during the experimental test (described in Section 2.3) were used. The diffuse solar irradiance was assumed to be isotropically distributed [34].

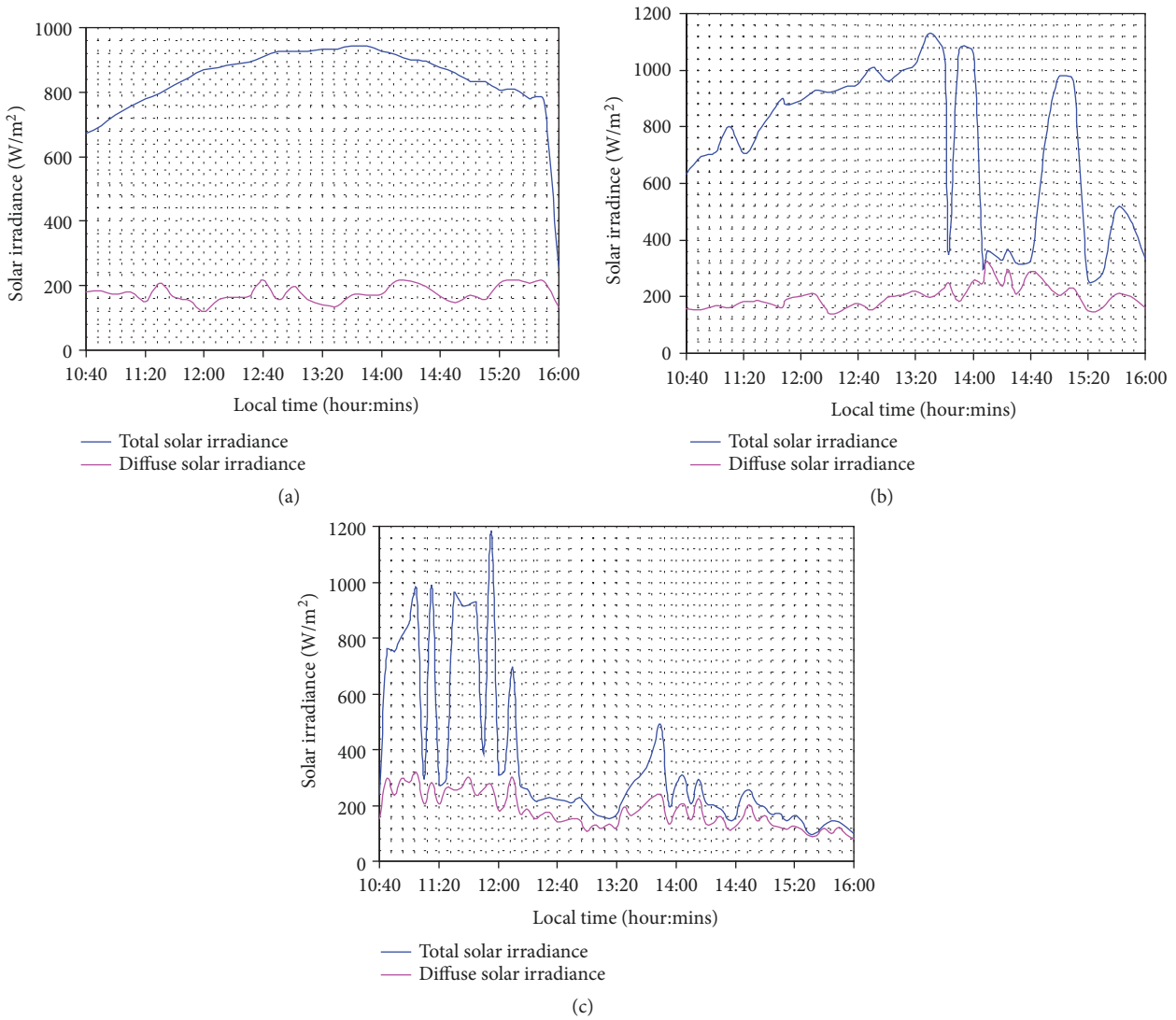

FIGURE 4: Variation of solar irradiance during experimental test: (a) clear sunny day, (b) partial cloudy day, and (c) overcast day, adapted from Paul and Smyth [28].

3. Results and Discussions

3.1. Solar Irradiance during Experimental Test. Figure 4 shows the variation of total and diffuse solar irradiance on the aperture of the CPC during the experimental test period. It can be seen that, during a clear sky day (Figure 4(a)), total solar irradiance was symmetrical and very high throughout the experimental test period. The maximum total solar irradiance was about 942 W/m^2 (around solar noon) and, due to high degree of the atmospheric transparency, the diffuse solar irradiance remained below 200 W/m^2 for most of the time of the experimental testing. With regard to partial cloudy day (Figure 4(b)), it can be seen that, due to clouds effect, the total solar irradiance before and after solar noon was not symmetrical and the value of the diffuse irradiance was always higher than 200 W/m^2 for most of the time. The total solar irradiance varied from about 260 W/m^2 to over 1,000 W/m^2. In analysing the performance of a PV cell with a concentrating system, the influence of clouds is an important parameter to consider because the presence of clouds in the sky decreases the amount of global solar irradiance and increases the amount of diffuse irradiance. Thus, in addition to a significant drop in the power output, the diffuse irradiance modifies the distribution profiles of the incident energy on the surface of the PV cell.

Figure 4(c) shows the variation of total and diffuse solar irradiance during the experimental test period on overcast day. Overcast weather differs from both clear sky and partial cloudy days in the sense that most of the time the incident solar irradiance is diffuse. It can be seen from Figure 4(c) that, before 12:20 hours, the weather condition was characterised by sunny-cloudy as illustrated by low and high total solar irradiance. For example, at 11:25 hours, the total solar irradiance was about 300 W/m^2 while at 11:55 hours it was over 1,000 W/m^2. However, between 12:15 and 16:00 hours, the sky was completely full of clouds as demonstrated

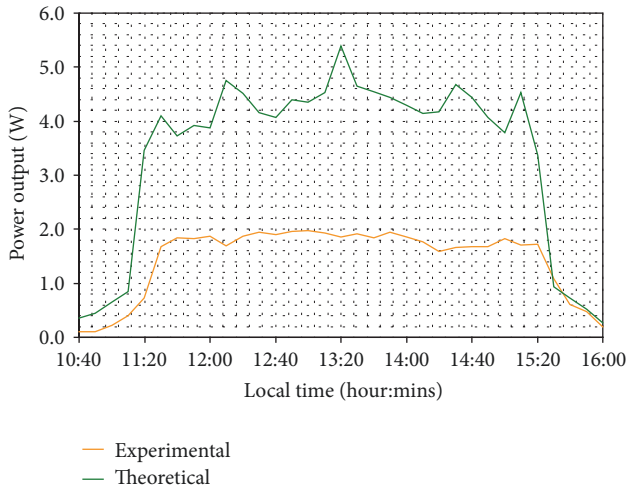

Figure 5: The comparison of experimental and theoretical power output for the hybrid PV cell on a clear sunny day.

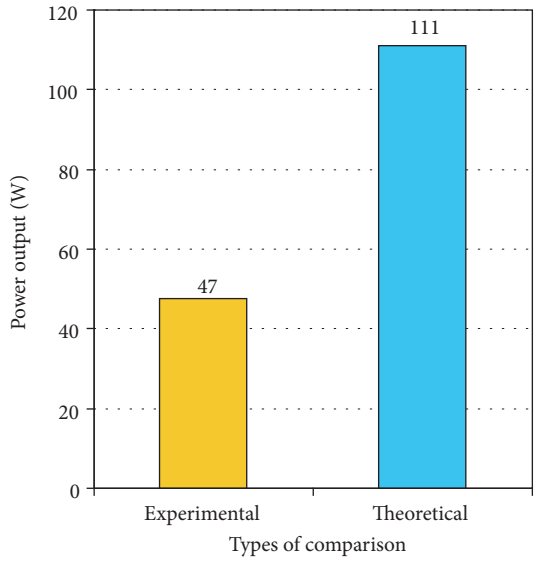

Figure 6: Power output produced by a hybrid PV cell over the test period on a clear sunny day.

by both low total solar irradiance and high diffuse irradiance. It was important to compare the theoretical and experimental power output for an overcast day because it has substantial impact on the power output of the hybrid PV cell (due to the fact most of the time the incident solar irradiance is diffuse).

3.2. Comparison of Experimental and Theoretical Power Output on a Clear Sunny Day. Figure 5 compares the experimental and theoretical power output produced by the hybrid PV cell on a clear sunny day. It can be seen that the theoretical power output was higher than the experimental values. However, the magnitude of discrepancy varied with the time of the day due to variations in solar irradiance. As illustrated in Figure 5, when the incidence angle of the solar irradiance was higher than the acceptance half–angle of the CPC, e.g., between 10:40 (θ_{in} = +40°) to 11:20 hours (θ_{in} = +32.5°) and 15:20 (θ_{in} = −32.5°) to 16:00 hours (θ_{in} = −40°), the variation between the experimental and theoretical power output was less compared to when the incidence angle of the solar irradiance was within the acceptance half–angle limits of the CPC, i.e., between 10:20 hours (θ_{in} = +30°) and 15:20 hours (θ_{in} = −30°). For example, at 11:10 hours (θ_{in} = +32.5°), the theoretical power output was higher than the experimental by about 110% whilst at 13:20 hours (θ_{in} = 0°) the difference was very high, about 190%. On the other hand, when the comparison was made based on the total time of the experimental test, i.e., from 10:40 to 16:00 hours (i.e., daily power output as presented in Figure 6), the power output obtained from experimental was 47 W compared to 111 W obtained by calculations, indicating about 136% increase in power output from theoretical results. The divergence of the experimental result from the theoretical was due to losses due to connecting wires series resistance effect, operating temperature effect, and the consequence of the optimal fixed resistive load. Previous studies have shown that maximum power output decreases due to series resistance effect [35, 36]. For example, van Dyk and Meyer [35] observed that an increase in series resistance (from 0.36 to 3.60 Ω) contributed to a power loss of 50% after outdoor exposure of 130 kWh/m^2. On the other hand, temperature increase has also a negative effect on the maximum power output of the solar cell [37, 38]. As indicated in Table 2 [32], the temperature coefficient for P_{MMP} is −0.49%/K, indicating that, for every 1°C (274.15K) above 25°C (298.15K), the maximum power output of the PV cell decreases by 0.49%.

It should be noted that none of these effects were taken into consideration in the calculations for the theoretical power output. However, it is the value of the optimal resistive load that had much impact on the experimental power output, especially when the incidence angle of the solar irradiance is within the acceptance half–angle limits of the CPC. This was the main reason why the power output was almost constant between 11:30 and 15:20 hours for experimental values whereas the theoretical power output increased with time until the maximum value was reached at solar noon, 13:20 hours (Figure 5). This is due to the fact that the value of the optimal resistive load used (102 mΩ) does not track well the power output below 500 W/m^2 and above 700 W/m^2 solar radiation intensities as illustrated in Figure 7. This is explained by the fact that resistive load method does not continuously adjust the electrical load to achieve the maximum possible power output as the irradiance varies through the day. This leads to maximum power output losses for solar irradiance outside the operating range of the optimal load value. Note that the results in Figure 7 were obtained by exposing the hybrid PV cell to different illumination intensities (300 to 1000 W/m^2) while recording current and voltage at each intensity level. The maximum power output with variable load method was obtained from the I-V curve measured by Keithley 2340 source-meter whereas the maximum power output with the optimal fixed resistive load was measured when the load value of 102 mΩ was incorporated in the experimental circuit diagram.

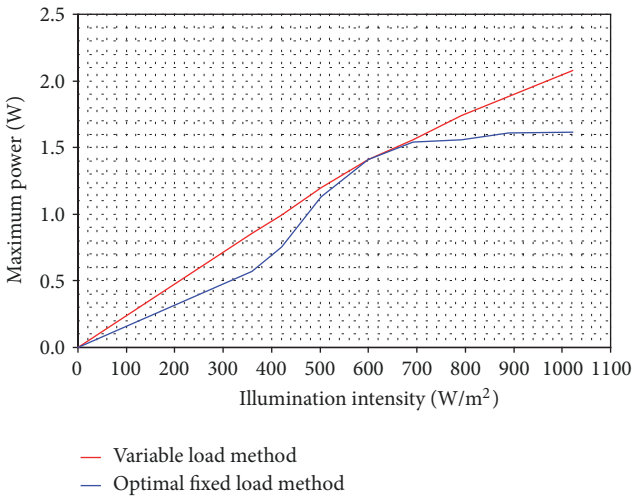

Figure 7: Variation of maximum power output of a hybrid PV cell as a function of optimal resistive load for different illumination intensities.

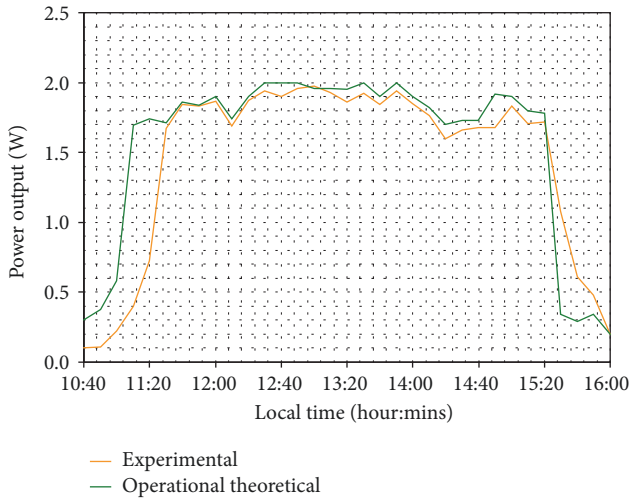

Figure 8: The comparison of the experimental and operational theoretical power output of the hybrid PV cell on a clear sky day.

To illustrate the effect of optimal resistive load on the experimental power output, theoretical power output was calculated based on the optimal resistive load value that was used during the experimental test. Such power output is termed as "operational theoretical power output". As an example, Figure 8 shows the variation of the experimental and operational theoretical power output of the hybrid PV cell on a clear sunny day. It can be seen that the experimental result was closer to the theoretical result due to incorporating the effect of optimal resistive load value in the calculations.

3.3. Comparison of Experimental and Theoretical Power Output on a Partial Cloudy Day. Figure 9 shows the comparisons of the experimental and theoretical power output of the hybrid PV cell on a partial cloudy day. It can be seen that the theoretical power output was higher than the experimental result, except from 15:30 to 16:00 hours. However,

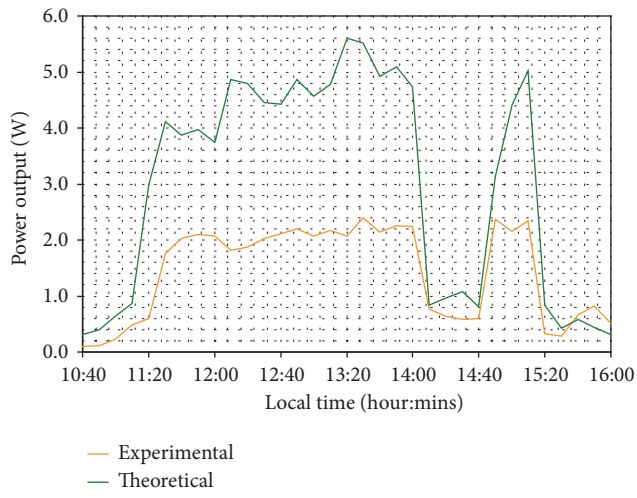

Figure 9: The comparison of experimental and theoretical power output of the hybrid PV cell on a partial cloudy day.

the magnitude varied with the amount of solar irradiance received. It was very high when the solar irradiance was high but very low when the solar irradiance was low. For example, the theoretical power output was higher than the experimental by about 110% with total solar irradiance of 950 W/m^2 (Figure 4(b)) at 13:20 hours while the difference was only about 39% with total solar irradiance of 330 W/m^2 (Figure 4(b)) at 14:40 hours. This is because optimal resistive load does not track well the P_{MPP} at higher solar irradiance as illustrated in Figure 7. In addition, power output loss was due to series resistance and rise in cell temperature effects.

To show the general variation between the experimental and theoretical power output for the whole day, instantaneous power output in Figure 9 was added together and the result is presented in Figure 10. It can be seen that the power output obtained experimentally was 47 W compared to 98 W obtained by calculations, indicating about 109% increase in power output from theoretical results. Again, this difference is explained by the losses due to connecting wires series resistance effect, operating cell temperature effect, and the effect of the fixed resistive load.

To examine further the effect of fixed resistive load on the experimental power output, the value of the resistive load was reduced from 102 mΩ to 45 mΩ. Similar experimental test as the one described in Section 2.3 was carried out during one of the partial cloudy days and the comparison of the results is presented in Table 3. It can be seen that the theoretical power output was higher than the experimental by about 194%. Therefore, there is a significant variation in the experimental power output when a load value of 45 mΩ was used instead of 102 mΩ. This is explained by the fact that the load value of 45 mΩ was not an optimal value as illustrated in Figure 11. As shown in Figure 11, the maximum power output of the PV produced with the load value of 45 mΩ does not correspond with that of the variable load method (which automatically adjusts the load as the solar irradiance varies throughout the day), except when the solar irradiance

Table 3: The comparison of experimental and theoretical daily power output of the hybrid PV cell when the load value of 45 mΩ was used instead of 102 mΩ.

Types of analysis	Daily power output (W)
Experimental	11.52
Theoretical	33.91
Difference (%)	*194.41*

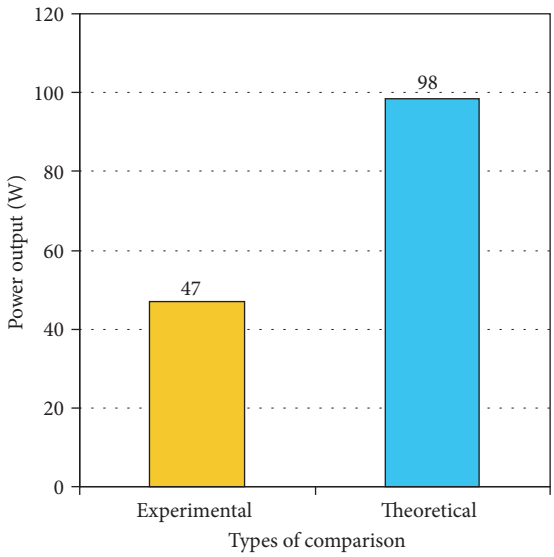

Figure 10: Power output produced by the hybrid PV cell over the entire test period on a partial cloudy day.

was 900 W/m^2. This results into maximum power output losses for solar irradiance below and above 900 W/m^2. It has been pointed out by Lasnier and Ang [19] that if the resistive load is smaller than the optimal value, the PV cell behaves as a constant current source (almost equal to the short-circuit current, independent of the voltage) which in turn causes nonlinear relationship between irradiance and output power and hence low output power.

3.4. Comparison of Experimental and Theoretical Power Output on Overcast Day. The variation of experimental and theoretical power output generated by a hybrid PV cell on overcast day is shown in Figure 12. It can be seen that although the value of theoretical power output was higher than the experimental value at any time, the difference was not as high as in Figure 5 (clear sky day) or Figure 9 (partial cloudy day). The difference was nearly constant through the experimental test period but the discrepancy between the theoretical and the experimental over the whole day was still very high (121%) as shown in Figure 13. This is due to the fact the experimental power output produced with a load value of 102 mΩ was nonlinear with solar irradiance at low intensities (below 500 W/m^2) as shown in Figure 7 hence low power output. The reason is that fixed resistive load does not automatically adjust the load to ensure maximum power output as the solar irradiance varies throughout the day.

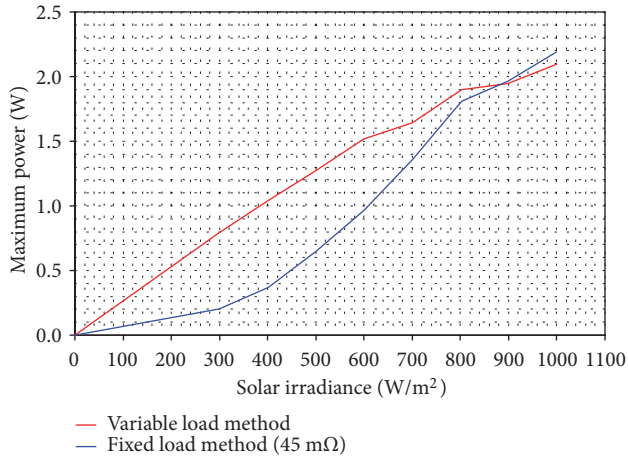

Figure 11: Variation of power output of the PV cell as a function of resistive load for different solar irradiance. The maximum power output with variable load method was obtained from the current versus voltage curve measured by Keithley 2340 source-meter while the power output with fixed resistive load was measured when the fixed load value of 45 mΩ was incorporated in the experimental circuit diagram.

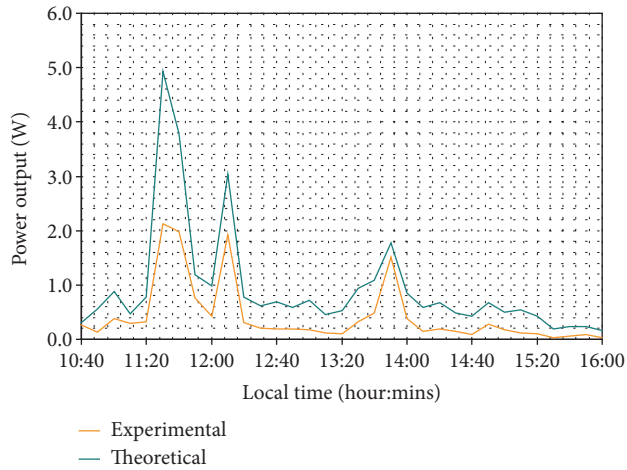

Figure 12: The comparison of experimental and theoretical power output for the hybrid cell on an overcast day.

4. Conclusion and Recommendation

In this paper, experimental and theoretical power output of a hybrid PV cell were analysed and compared for three different weather conditions (clear sky, partial cloudy, and overcast days). The hybrid PV cell consisted of mono-crystalline solar cell of 12% as low efficiency cell and strips of Bosch M 2BB mono-crystalline cell (17.5%) as high efficiency cell. The current and voltage for the experimental results were measured by using a fixed resistive load method. Theoretical daily power output was calculated based on the hourly incident energy on each section, the size of the section, and the electrical conversion efficiency of each section of the hybrid cell. The hybrid cell was evaluated within a low-concentrating symmetric 2D CPC suitable for building integration and was

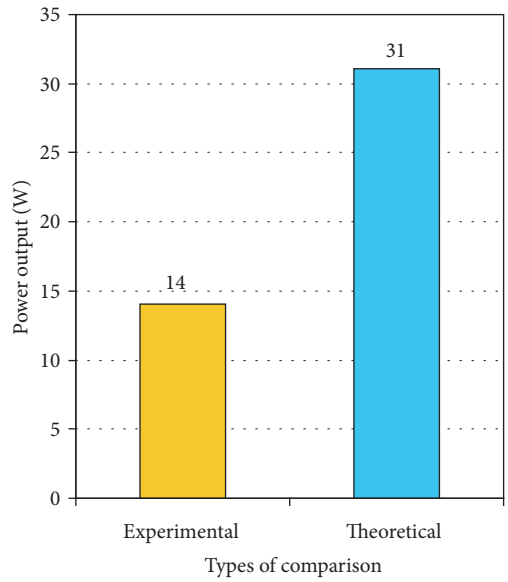

Figure 13: Power output produced by a hybrid PV cell for the whole day on an overcast day.

tilted at 54°. It was found that the theoretical daily power output on a clear sky day, partial cloudy day, and overcast day was higher than the experimental result by 136%, 109%, and 121%, respectively. The discrepancy was due to losses as the result of connecting wires series resistance effect, operating temperature effect, and the consequence of the fixed resistive load. These effects were not taken into consideration in the calculations for the theoretical power output. However, it was the value of the optimal fixed resistive load that had much impact on the experimental power output, especially when the incidence angle of the solar irradiance was within the acceptance half–angle limits of the CPC. This was due to the fact that the use of optimal load method does not automatically adjust the load as the solar irradiance varies throughout the day. Therefore, this has confirmed that the proposed hybrid PV cell is cable of generating high power output.

Since the use of optimal resistive load method was found to limit the values of the experimental power output, it is recommended that a data acquisition system such as PV Peak Power Measuring Device 6020C or Keithley 2651A source-meter which is capable of measuring high current value should be used. It is also recommended that when simulation analysis is used, it should take into consideration all the factors that affect the power output of the PV cell such as connecting wires series resistance and operating cell temperature.

Nomenclature

A_i: Area of the *i*th section of a PV cell [m^2]
C_B: Beam energy concentration [-]
C_D: Diffuse energy concentration [-]
G_B: Beam solar irradiance on the aperture of the CPC [W/m^2]
G_D: Diffuse solar irradiance on the aperture of the CPC [W/m^2]
I_{MPP}: Current at the maximum power point [A]
I_{SC}: Short–circuit current [A]
P_{Daily}: Total daily electrical energy produced by a PV cell [Wh]
P_{Hour}: Hourly electrical power output of the hybrid PV cell [W]
$P_{Hour}(i)$: Hourly electrical power output of the *i*th section of a PV cell [W]
P_{MPP}: Power output at maximum power point [W]
V_{MPP}: Voltage at the maximum power point [V]
V_{OC}: Open–circuit voltage [V]
i-index: *i*th section of the hybrid PV cell [-].

Greek

α: Temperature coefficient of the short–circuit current [%/K]
β: Temperature coefficient of the open–circuit voltage [%/K]
γ: Temperature coefficient of the power output at maximum power point [%/K]
η: Solar cell conversion efficiency [-]
η_i: Electrical conversion efficiency of the *i*th section of a PV cell [-]
θ_a: Acceptance half-angle [°].

Abbreviations

2D: Two-dimensional
AM: Air mass
CPC: Compound parabolic concentrator
HE: High efficiency
I-V: Current against voltage
LE: Low efficiency
PV: Photovoltaic.

Data Availability

The data used to support the findings of this study are available from the corresponding author upon request.

Disclosure

Current address of Damasen Ikwaba Paul is Department of Electrical Engineering, College of Engineering, Chosun University, 309, Pilmun-daero, Dong-gu, Gwangju 501-759, Republic of Korea. Permanent address of Damasen Ikwaba Paul is Faculty of Science, Technology and Environmental Studies, The Open University of Tanzania, P.O. Box 23409, Dar es Salaam, Tanzania.

Conflicts of Interest

The author declares that there are no conflicts of interest.

Acknowledgments

The author wishes to thank Chosun University (Republic of Korea) for their financial support. Indeed, without this funding, this article would have not been written.

References

[1] M. Z. Jacobson, "Review of solutions to global warming, air pollution, and energy security," *Energy & Environmental Science*, vol. 2, no. 2, pp. 148–173, 2009.

[2] J. O. Petinrin and M. Shaaban, "Renewable energy for continuous energy sustainability in Malaysia," *Renewable & Sustainable Energy Reviews*, vol. 50, pp. 967–981, 2015.

[3] E. Kabir, P. Kumar, S. Kumar, A. A. Adelodun, and K.-H. Kim, "Solar energy: potential and future prospects," *Renewable & Sustainable Energy Reviews*, vol. 82, pp. 894–900, 2018.

[4] A. Goetzberger, C. Hebling, and H. Schock, "Photovoltaic materials, history, status and outlook," *Materials Science and Engineering: R: Reports*, vol. 40, no. 1, pp. 1–46, 2003.

[5] G. M. Masters, *Renewable and Efficient Electric Power Systems*, John Wiley & Sons, Inc., Hoboken, NJ, USA, 2004.

[6] D. J. Chen, *Physics of Solar Energy*, John Wiley and Sons, Inc., New Jersey, NJ, USA, 2012.

[7] T. K. Mallick, P. C. Eames, T. J. Hyde, and B. Norton, "The design and experimental characterisation of an asymmetric compound parabolic photovoltaic concentrator for building façade integration in the UK," *Solar Energy*, vol. 77, no. 3, pp. 319–327, 2004.

[8] E. Durán, J. M. Andújar, J. M. Enrique, and J. M. Pérez-Oria, "Determination of PV generator *I-V/P-V* characteristic curves using a DC-DC converter controlled by a virtual instrument," *International Journal of Photoenergy*, vol. 2012, Article ID 843185, 13 pages, 2012.

[9] D. I. Paul, M. Smyth, A. Zacharopoulos, and J. Mondol, "The design, fabrication and indoor experimental characterisation of an isolated cell photovoltaic module," *Solar Energy*, vol. 88, pp. 1–12, 2013.

[10] S. Fanourakis, K. Wang, P. McCarthy, and L. Jiao, "Low-cost data acquisition systems for photovoltaic system monitoring and usage statistics," *IOP Conference Series: Earth and Environmental Science*, vol. 93, Article ID 012048, 2017.

[11] H. Rezk, I. Tyukhov, M. Al-Dhaifallah, and A. Tikhonov, "Performance of data acquisition system for monitoring PV system parameters," *Measurement*, vol. 104, pp. 204–211, 2017.

[12] E. Duran, M. Piliougine, M. Sidrach-de-Cardona, J. Galan, and J. Andujar, "Different methods to obtain the I–V curve of PV modules: a review," in *Proceedings of the 33rd IEEE Photovoltaic Specialists Conference (PVSC'08)*, pp. 1–6, San Diego, CA, USA, May 2008.

[13] E. E. Van Dyk, A. R. Gxasheka, and E. L. Meyer, "Monitoring current-voltage characteristics of photovoltaic modules," in *Proceedings of the 29th IEEE Photovoltaic Specialists Conference*, pp. 1516–1519, USA, May 2002.

[14] E. E. Van Dyk, A. R. Gxasheka, and E. L. Meyer, "Monitoring current-voltage characteristics and energy output of silicon photovoltaic modules," *Journal of Renewable Energy*, vol. 30, no. 3, pp. 399–411, 2005.

[15] A. Q. Malik and S. J. B. H. Damit, "Outdoor testing of single crystal silicon solar cells," *Journal of Renewable Energy*, vol. 28, no. 9, pp. 1433–1445, 2003.

[16] M. M. Mahmoud, "Transient analysis of a PV power generator charging a capacitor for measurement of the I–V characteristics," *Journal of Renewable Energy*, vol. 31, no. 13, pp. 2198–2206, 2006.

[17] A. B. Rao and G. R. Padmanabhan, "A method for estimating the optimum load resistance of a silicon solar cell used in terrestrial power applications," *Solar Energy*, vol. 15, no. 2, pp. 171–177, 1973.

[18] C. R. Osterwald, J. Adelstein, J. A. Del Cueto et al., "Resistive loading of photovoltaic modules and arrays for long-term exposure testing," *Progress in Photovoltaics*, vol. 14, no. 6, pp. 567–575, 2006.

[19] F. Lasnier and T. Ang, *Photovoltaic Engineering Handbook*, Adam Hilger, Bristol, UK, 1990.

[20] E. R. Messmer, "Solar cell efficiency vs. module power output: simulation of a solar cell in a CPV module," in *Solar Cells - Research and Application Perspectives*, A. Morales-Acevedo, Ed., pp. 308–326, IntechOpen Limited, London, UK, 2013.

[21] A. Q. Jakhrani, S. R. Samo, S. A. Kamboh, J. Labadin, and A. R. H. Rigit, "An improved mathematical model for computing power output of solar photovoltaic modules," *International Journal of Photoenergy*, vol. 2014, Article ID 346704, 9 pages, 2014.

[22] A. Shukla, M. Khare, and K. N. Shukla, "Modeling and simulation of solar PV module on MATLAB/simulink," *International Journal of Innovative Research in Science, Engineering and Technology*, vol. 4, no. 1, pp. 18516–18527, 2015.

[23] J. Cubas, S. Pindado, and F. Sorribes-Palmer, "Analytical calculation of photovoltaic systems maximum power point (MPP) based on the operation point," *Applied Sciences*, vol. 7, no. 9, p. 870, 2017.

[24] C. I. Wade, R. Torihara, T. Sakoda, and N. Hayashi, "Numerical analysis of electrical characteristics of a PV module irradiated by an impulse light flash," *Journal of International Council on Electrical Engineering*, vol. 8, no. 1, pp. 8–13, 2018.

[25] J. Banks, "Introduction to simulation," in *Proceedings of the 1999 Winter Simulation Conference (WSC '99)*, vol. 11, pp. 7–13, 1999.

[26] R. Shannon, "Introduction to the art and science of simulation," in *Proceedings of the IEEE Winter Simulation Conference (WSC'98)*, vol. 11, pp. 7–14, Washington, DC, USA, 1998.

[27] D. I. Paul, "Application of compound parabolic concentrators to solar photovoltaic conversion: a comprehensive review," *International Journal of Energy Research*, pp. 1–48, 2019.

[28] D. I. Paul and M. Smyth, "Enhancing the performance of a building integrated compound parabolic photovoltaic concentrator using a hybrid photovoltaic cell," *International Journal of Renewable Energy Technology*, 2019.

[29] D. Chemisana, "Building integrated concentrating photovoltaics: a review," *Renewable & Sustainable Energy Reviews*, vol. 15, no. 1, pp. 603–611, 2011.

[30] D. I. Paul, "Optical performance analysis and design optimisation of multisectioned compound parabolic concentrators for photovoltaics application," *International Journal of Energy Research*, vol. 43, no. 1, pp. 358–378, 2018.

[31] Anon, "Mono-crystalline PV cell technical data sheet," Tech. Rep., Bluesky Led Technology Co., Ltd., HangZhou, China, 2010.

[32] Anon, "High performance – stable yield," Tech. Rep., Bosch Solar Cell M 2BB, Bosch Solar Energy AG Wilhelm-Wolff-Straße 23 99099, Erfurt, Germany, 2010.

[33] A. Zacharopoulos, *Optical design modelling and experimental characterisation of line-axis concentrators for solar photovoltaic*

and thermal applications, [Ph.D. thesis], University of Ulster, UK.

[34] D. E. Prapas, B. Norton, and S. D. Probert, "Thermal design of compound parabolic concentrating solar-energy collectors," *Journal of Solar Energy Engineering*, vol. 109, no. 2, pp. 161–168, 1987.

[35] E. E. van Dyk and E. L. Meyer, "Analysis of the effect of parasitic resistances on the performance of photovoltaic modules," *Journal of Renewable Energy*, vol. 29, no. 3, pp. 333–344, 2004.

[36] R. Singh, B. Bora, K. Yadav et al., "Effect of series resistance on degradation of isc, power output and fill factor of HIT technology," in *Proceedings of the 2015 IEEE 42nd Photovoltaic Specialists Conference (PVSC)*, pp. 1–5, New Orleans, LA, USA, June 2015.

[37] A. Royne, C. J. Dey, and D. R. Mills, "Cooling of photovoltaic cells under concentrated illumination: a critical review," *Solar Energy Materials & Solar Cells*, vol. 86, no. 4, pp. 451–483, 2005.

[38] D. I. Paul, M. Smyth, and A. Zacharopoulos, "The effect of non-uniformities in temperature on the performance parameters of an isolated cell photovoltaic module with a compound parabolic concentrator," *International Journal of Renewable Energy Technology*, vol. 10, no. 1/2, pp. 3–25, 2019.